Journal of Medicinal Chemistry

Fragment based optimization of metabotropic glutamate receptor-2 (mGluR2) positive allosteric modulators in the absence of structural information

György Szabó, György István Túrós, Sándor Kolok, Mónika Vastag, Zsuzsanna Sánta, Miklós Dékány, György I. Lévay, István Greiner, Minami Natsumi, Watanabe Tatsuya, and Gyorgy M. Keseru

J. Med. Chem., **Just Accepted Manuscript** • DOI: 10.1021/acs.jmedchem.8b00161 • Publication Date (Web): 05 Mar 2018

ACS Publications

is published by the American Chemical Society. 1155 Sixteenth Street N.W., Washington, DC 20036

Fragment based optimization of metabotropic glutamate receptor-2 (mGluR2) positive allosteric modulators in the absence of structural information

György Szabó,[1] György I. Túrós,[1] Sándor Kolok,[1] Mónika Vastag,[1] Zsuzsanna Sánta,[1] Miklós Dékány,[1] György I. Lévay,[1] István Greiner,[1] Minami Natsumi,[3] Watanabe Tatsuya,[3] György M. Keserű*[2]*

[1]Gedeon Richter Plc., 19-21 Gyömrői út, Budapest, 1103 Hungary

[2]Medicinal Chemistry Research Group, Research Centre for Natural Sciences, Hungarian Academy of Sciences, 2 Magyar tudósok körútja, Budapest 1117 Hungary

[3]Mitsubishi Tanabe Pharma Corporation, 1000, Kamoshida-cho, Aoba-ku, Yokohama 227-0033, Japan

ABSTRACT

Metabotropic glutamate receptor 2 (mGluR2) positive allosteric modulators (PAMs) have been implicated as potential pharmacotherapy for psychiatric conditions. Screening our corporate compound deck, we identified a benzotriazole fragment (**4**) that was rapidly optimized to a potent and metabolically stable early lead (**16**). The highly lipophilic character of **16**, together with its limited solubility, permeability and high protein binding, however, did not allow to reach

the proof of concept *in vivo*. Since further attempts on the optimization of druglike properties were unsuccessful, the original hit **4** has been revisited and was optimized following the principles of fragment based drug discovery (FBDD). Lacking structural information of the receptor-ligand complex we implemented a group efficiency (GE) based strategy and identified a new fragment like lead (**60**) with more balanced profile. Significant improvement achieved on the druglike properties nominated the compound for *in vivo* proof of concept studies that revealed the chemotype being a promising PAM lead targeting mGluR2 receptors.

INTRODUCTION

The family of metabotropic glutamate receptors (mGlu1-8) is classified into three groups based on structural homology, transduction mechanisms, and pharmacology.[1] Group II metabotropic receptors include mGluR2 and mGluR3 which are highly homologous (~70% at the amino acid level) and linked to their effectors via Gi/o proteins (e.g. suppression of adenylate cyclase when expressed in cell lines). The mGluR2/3 receptors are localized widely throughout the brain in circuits of relevance for neuropsychiatric disorders, such as the neocortex, thalamus, striatum, amygdala and hippocampus.[2] Functionally, activation of mGluR2/3 receptors *in vivo* suppresses enhanced synaptic excitability via inhibition of presynaptic glutamate release and postsynaptic activation of potassium channels that control neuronal hyperpolarization.[3] In general, mGluR2/3 receptors have a predominant extrasynaptic localization. Thus, mGluR2/3 receptors provide a negative feedback to keep glutamate transmission within the physiological range and thus prevent hyperexcitability from interfering with normal brain function.

According to the glutamatergic hypothesis of schizophrenia, hyperactivity of glutamatergic transmission in the limbic regions is the underlying mechanism in the pathogenesis of schizophrenia. It has been postulated that agonists at mGluR2/3 receptors could decrease schizophrenic symptoms by reducing transmission at glutamatergic synapses and thus they might represent a novel non-dopaminergic strategy for the treatment of schizophrenia.[4] The antipsychotic properties of mGluR2/3 receptor agonists are supported by broad range of preclinical data.[5] In studies using transgenic mice lacking the mGluR2 or mGluR3 receptor, it has been shown that the antipsychotic effects of the mGluR2/3 receptor agonists in the models of psychosis are mediated through the activation of mGluR2 and not of mGluR3 receptors.[6] Moreover, the Phase II clinical trial of LY2140023 (**1**), a selective mGluR2/3 receptor agonist

(Figure 1), showed efficacy on schizophrenic subjects. It has been shown to improve positive symptoms in patients thus being comparable with olanzapine, but it has not been shown to produce any prolactin elevation, extrapyramidal symptoms or weight gain.[7] However, in 2012, Eli Lilly announced to stop Phase III development as **1** failed to meet its primary endpoint based on the unaltered PANSS scale.[8,9]

One alternative approach to direct-acting mGluR2 receptor agonists is the use of subtype-selective PAMs. These ligands do not activate the mGluR2 *per se* but act at an allosteric binding site to potentiate glutamate-induced activation of this receptor. Since a potentiator with no inherent agonist activity would only function in the presence of the endogenous agonist, the receptor would not be activated continuously, avoiding receptor desensitization which often occurs after repeated dosing of orthosteric agonists.[10] In addition, the allosteric binding sites on glutamate receptors might sufficiently be different as to make subgroup selectivity feasible.[11]

Over the last decade a large number of structurally different chemotypes have been disclosed and reviewed.[12] To date, two mGluR2 PAM molecules have reached the clinic (Figure 1). AZD8529 (**2**) had been in phase II clinical trial at AstraZeneca in schizophrenic patients; however further development was halted in 2011 due to a lack of efficacy.[13]

ADX71149 (**3**), also known as JNJ-40411813, was investigated by Addex Therapeutics and Janssen Pharmaceuticals for the treatment of schizophrenia[14] and anxious depression (major depressive disorder with anxiety symptoms).[15] In a phase IIa study **3** was well tolerated and showed promising effects in schizophrenia patients but was not effective in patients with major depressive disorder and anxiety.[16]

Our efforts in the field of mGluR2 PAMs started with a functional screen of our corporate compound collection. The benzyl substituted benzotriazole derivative **4** was identified from this campaign as an attractive small molecule with low micromolar activity (mGluR2 PAM EC_{50} = 3 μM, Figure 2). These data confirmed that **4** is a much smaller (N_{hev}=16) but still potent compound with higher ligand efficiency (LE=0.49) as compared to known mGluR2 PAMs[12] (average Nhev=29±4; average LE=0.25±0.4) that validates it for follow-up studies. Freedom to operate analysis identified only a 5-disubstituted benzotriazole series of Merck[17-19] that was subjected to detailed evaluation. In contrast to **4** the patent describes complex drug-like compounds all having large substituents at position 5. Interestingly other positions of the core were much less elaborated. This observation prompted us to explore the potential growing vectors around the benzotriazole core systematically. This work has been started by the analysis of the available pharmacophore model.[20] Aligning our fragment like hit (**4**) to larger mGluR2 PAMs we identified the primary growing vectors and rapidly converted 4 to the biaryl derivative **5**, that resulted in substantial improvement in mGluR2 PAM potency (mGluR2 PAM EC_{50} = 155 nM). Although incorporation of the biaryl-ring system increased the lipophilicity, we were encouraged by the relative balance between mGlu2 PAM potency and ligand efficiency (LE = 0.44) compared to the original hit **4** (Figure 2). As **5** showed virtually the same low metabolic stability on human, rat and mouse microsomes, our primary objective was to improve metabolic stability, while maintaining the target potency and ligand efficiency of novel benzotriazole derivatives. We herein report the successful optimization of benzotriazoles which led to the identification of the advanced lead **60**. This "fragment-like" molecule showed good mGluR2 receptor PAM in vitro activity, ADME and PK profile with reasonable activity in the PCP-induced hyperlocomotion and DOI-induced head twitch models of psychosis.

RESULTS

Chemistry. The general synthesis of unsubstituted benzotriazole target compounds **5**, **10-19** are shown in Scheme 1. Reaction of commercially available benzotriazole **6** with the appropriate bromobenzyl derivatives **7** in THF using NaHMDS provided the key bromoaryl intermediates **8**. Target compounds **10-19** were prepared via Suzuki-coupling of **8** with the corresponding boronic acids **9**. The chemical structures of **10-19** are shown in Table 1 and 3.

Substituted benzotriazoles **24-60** were prepared following the synthesis sequence shown in Scheme 2. Treatment of 1-fluoro-2-nitrobenzene derivatives **20** with aminomethyl derivatives **21** afforded nitroanilines **22**. Reduction of **22** in the presence of $SnCl_2$ in $MeOH/H_2O$ yielded dianilines **23** that were cyclized to the final benzoriazole compounds **24-60** in AcOH using $NaNO_2$. The chemical structures of **24-60** are shown in Table 4, 5 and 6.

Medicinal chemistry optimization of the HTS hit (4). Functional screening of our corporate library on mGluR2 overexpressing cells resulted in a benzyl-benzotriazole singleton with acceptable potency and high ligand efficiency. Structural alignment with known mGluR2 PAM reference compounds revealed that there are two potential growing vectors available; one at position 4 of the benzotriazole core and another at the para position of the benzyl group (Figure 2). Our first attempts were focused towards the latter vector and tried to improve the metabolic stability of the biaryl-benzotriazole advanced hit **5** by exploring different substituents of the terminal phenyl ring along vector 1 (**10-19)**. Literature data[21] suggested that 2, 4-disubstitution in this region is beneficial for potency. A representative set of analogues to exemplify the SAR trends identified is shown in Table 1. Overall, dual substitution at positions 2 and 4 gave

compounds (**10-15**) with improved potency and metabolic stability out of which compound **11** showed the best profile. Since the highly lipophilic character of the compounds resulted in limited solubility we next introduced ring nitrogens (**16-19**). Compound **16** showed reasonable potency and metabolic stability with somewhat improved lipophilicity that nominated the compound as an early lead.

Compound **16** was next subjected to extended profiling that included its investigations in a broad panel of receptors, ADME assays, *in vivo* pharmacokinetics and *in vivo* efficacy models (Table 2).

Characterization of **16** showed that the compound has promising off target profile. Although the kinetic solubility was still limited and plasma protein binding was considerably high, other ADME parameters were found to be acceptable and the compound progressed to *in vivo* studies. Mouse pharmacokinetics data suggested limited exposures (C_{plasma}: 2.0 μM, C_{brain}: 1.4 μM, $C_{plasma\ unbound}$: 0.015 μM) for **16** and consequently the compound did not show efficacy in the PCP-induced hyperlocomotion model (PCP HL ED_{50} > 100 mg/kg, i.p.). On the basis of the *in vivo* data we concluded that further improvement in potency and ADME properties are needed to realize the desired *in vivo* efficacy in disease models. To achieve this goal, we next tested the effect of substituents towards the other growing vector (vector 2, Figure 2). A fluoro scan around the benzotriazole core revealed that position 4 is beneficial for the potency that was further optimized to compound **29** having single digit nanomolar potency and acceptable metabolic stability (Table 3).

Unfortunately, however, the improvement in potency was associated with significant increase in lipophilicity that turned the druglike properties of **29** less than optimal. Pharmacokinetic investigation of this compound revealed that **29** reached improved plasma and brain levels after

30 mg/kg oral dose in mice (C_{plasma}: 20 μM, C_{brain}: 7.1 μM, $C_{plasma\ unbound}$: 0.081 μM) but these exposures resulted in only limited improvement in the PCP-induced hyperlocomotion model (PCP HL ED_{50}: 47 mg/kg, i.p.). Any further attempt of decreasing lipophilicity resulted in significant drop in potency. Therefore, we decided to revisit the original hit **4** and tried its optimization following fragment based drug discovery principles.

Fragment based optimization of the HTS hit (4). Most of the successful fragment based drug discovery programs rely on structural information typically from X-ray and/or NMR studies of ligand-protein complexes.[23] Fragment optimization strategies, such as growing, merging and linking require this information to improve the binding affinity while controlling the physicochemical properties. Although there is an increasing number of membrane protein structures available in PDB, mGluR1 and mGluR5, members of Group I mGluRs are the only representatives of class C GPCRs. MGluR2 belongs to Group II and furthermore the present PAM program requires its active conformation that is not available for any class C GPCRs. Consequently, computational models of protein-ligand complexes might fail to identify the correct binding mode and grow vectors and therefore could not be used to drive the optimization. There is a consensus that in the lack of structural information, fragment optimizations are challenging. Identification of growing vectors, however, can be feasible with structure activity relationship (SAR) information. Without prior knowledge, all positions around the fragment core have equal chance for growing or need for modifications. One of the possible strategies of using SAR information is based on LE, suggesting that only derivatives with LE larger than 0.4 are suitable for growing while less ligand efficient analogues the positions of substituents should be further optimized. Tactically, one should keep or increase LE during growing with the

simultaneous control of lipophilic measures such as LLE_{at} or LELP.[24] The other strategy is based in the group efficiency (GE) concept.[25] This methodology assumes that the molecules being compared bind in a similar fashion and evaluates the relative contribution of structural moieties to the binding free energy. Synthesizing and testing a number of close analogues around the fragment core the contributions of the individual substituents can be evaluated and positions by the lowest GE selected for subsequent modification.[26] Here we implemented the latter methodology and analyzed the GEs of compound **29** (Figure 3).

GE analysis of **29** revealed that we should keep the benzotriazole core with the bromine substituent at position 4. The biaryl part of the structure, however, adds less to the binding free energy and therefore we selected this part for modification. Removal of the 2-fluoro-4-chlorophenyl group in **29** to give **30** resulted in a significant reduction in potency, which was more than compensated by the reduced size and overall resulted in an improved LE value from 0.47 to 0.59. Additionally, **30** with a bromine substituent at position 4 showed a marked increase in potency as we compare to the original hit (**4**) (Table 4). It was clear from these data that the main pharmacophore for mGluR2 PAM activity included the 4-bromo benzotriazole core and we should focus our efforts on improving the mGluR2 PAM potency and most importantly the metabolic stability of this ring system. Our strategy was to optimize the substituents of the benzyl part of **30** without growing the molecule substantially (Table 4).

Fluoro scan around the benzyl group suggested position 4 as the most promising. This is in line with growth vector 1 used in the original optimization, however, compound **33** is about 10 times more potent than **5** and more importantly its ligand efficiency and lipophilicity is much more beneficial than that of the earlier advanced hit **5**. Interestingly, unlike the case of **5** and derivatives dual substitution at positions 2 and 4 did not improve the potency further. Next we

tried to decrease the lipophilicity of the compounds by the insertion of nitrogens to the benzyl ring (**39-41**) but the potency was substantially decreased. Continuing our efforts on the reduction of the lipophilicity we replaced the benzyl group of **30** by a number of alkyl and cycloalkyl substituents (Table 5).

Both alkyl and cycloalkyl side-chains decreased lipophilicity but made the compounds metabolically vulnerable. On the other hand, cycloalkyl substituents (**42-45**) improved the potency. Compound **45** showed reasonable potency with acceptable metabolic stability except for that measured by mouse microsomes. We therefore selected this compound for further optimization. During the final round of our medicinal chemistry program we fine-tuned the substituents along vector 2 (Table 6).

To improve metabolic stability of **45** we explored position 6 by introducing a range of substituents (**51-55**). Larger substituents such as trifluoromethyl (**51**), methoxy (**55**) groups and also fluorine (**54**) decreased the potency as compared to other halogens (**52**, **53**) but no significant improvement in mouse metabolic stability was observed. Finally, we tested the effect of different substituents at position 4 (**56-60**). In general, the compounds showed much lower potency relative to the corresponding bromine derivative **45** except for the chlorine (**56**) and the trifluoromethyl (**60**) analogue of which the latter was considered as a lead with balanced potency and metabolic profile. Compound **60** has therefore been further profiled on extended ADME screens that showed improved properties in solubility, permeability and plasma protein binding as compared to **16** (Table 2). Its improved profile has been reflected in the pharmacokinetics data, more specifically in brain levels (mouse Cplasma: 12.1 μM, Cbrain: 13.1 μM, Cplasma unbound: 1.75 μM after 30 mg/kg oral dosing) and also *in vivo* results as compound **60** showed

significant improvement in both the PCP-induced hyperlocomotion and the DOI-induced head twitch models (Figure 4).

DISCUSSION AND CONCLUSIONS

Here we report the optimization of a mGluR2 PAM screening hit (**4**) by standard medicinal chemistry and fragment based drug discovery (FBDD) principles. Since **4** was a moderately potent compound with limited metabolic stability our first attempts were focused improving these features. As a result, routine optimization of the screening hits resulted in a potent and metabolically stable early lead (**16**). Characterization of the druglike properties of **16**, however, revealed that the compound has limited solubility and permeability and high plasma protein binding. In line with these properties **16** showed limited exposures in the subsequent pharmacokinetic study and it failed to demonstrate efficacy in the PCP-induced hyperlocomotion test, one of the proof of concept *in vivo* models. Since further attempts on the optimization of druglike properties were unsuccessful, the chemistry program has been restarted and we decided to optimize **4** using the principles of fragment based drug discovery. The lack of structural information on the target, however, represented a significant challenge in the FBDD program. Implementing the group efficiency based strategy[22] together with several rounds of substituent scans we were able to identify a series of analogues with reasonable potency and improved druglike properties. This work highlighted some interesting features of the benzotriazole type mGluR2 PAMs. Systematic exploration of the SAR around the core revealed new growing vectors. Consequently, substituents at position 5 are not needed to achieve the target potency. Instead, we identified multiple substitution patterns providing novel compounds with high mGluR2 PAM efficacy. Furthermore, we demonstrated for the first time that single digit nanomolar mGluR2 PAM potency can be realized by fragments. In due course we identified a set

of mGluR2 PAMs with extremely high ligand efficiency indicating that the receptor can be efficiently activated via fragments not only at the orthosteric but also at the allosteric site. Careful fragment based optimization of the initial hit (**4**) finally led to **60** that still keeps the fragment features. The balanced profile of **60** nominated this compound for *in vivo* pharmacokinetic studies that revealed its significantly higher brain exposures compared to **16**. Due to its improved PK profile the compound was found to be effective in both of our proof of concept animal models having ED_{50} values of 37.6 and 29.7 mg/kg in PCP-induced hyperlocomotion and DOI-induced head twitch tests, respectively. The successful FBDD strategy used for the identification of **60** provideed a suitable tool for studying the therapeutical significance of mGluR2 PAMs and also demonstrated the feasibility of group efficiency driven FBDD approaches in the lack of structural information.

EXPERIMENTAL SECTION

General experimental methods. All reactions were carried out under dry nitrogen. Commercially available reagents were used without further purification. Solvents and gases were dried according to standard procedures. Organic solvents were evaporated with reduced pressure using a rotary evaporator. Purity of final compounds was verified using a Merck-Hitachi Lachrom Elite HPLC system. A linear gradient using water and 0.1% TFA (solvent A) and acetonitrile and 0.1% TFA (solvent B); t = 0 min, 0% B, t = 7.5 min, 70% B, t = 9.7 min, 90% B, t = 12.5 min, 90% B (12.5 min) was employed on Chromolith RP18e (3 x 100 mm) column. The flow rate was set to 1.7 mL/min and the column was maintained at 40 ^{o}C. Purity of final compounds was assessed using UV detection (Diode Arry Detector: Merck-Hitachi Lachrom Elite L-2450) at 215 nm; all tested compounds were ≥ 95% pure. NMR spectra were recorded at

298K either on an Agilent (Varian) NMRS-500 spectrometer (^{1}H: 499.9 MHz; ^{13}C: 125.7 MHz) equipped with a HCN 5mm PFG Triple Resonance ^{13}C Enhanced Cold Probe or on an Agilent (Varian) NMRS-400 (^{1}H: 399.8 MHz) equipped with a ^{1}H-^{19}F/^{15}N-^{31}P 5mm PFG OneNMR Probe or on an Agilent (Varian) NMRS-800 (^{1}H: 799.7 MHz; ^{13}C: 201.0 MHz) equipped with a HCN 5mm PFG Triple Resonance ^{13}C Enhanced Salt Tolerant Cold Probe using DMSO-d_6 as solvent if not stated otherwise. Four of the samples (marked with *****) were measured on a Bruker Avance III HDX 500 spectrometer (^{1}H: 499.9 MHz; ^{13}C: 125.7 MHz) using DMSO-h_6:DMSO-d_6 1:5 as solvent, therefore presaturation was used for solvent suppression. ^{1}H and ^{13}C chemical shifts were referenced to TMS. ^{15}N chemical shifts were determined from ^{1}H,^{15}N-HMBC spectra and are referenced to nitromethane by internal autocalibration method of the software.

EI-MS analysis was performed on a Finnigan MAT 95 XP system. The ionization method was EI and operated in positive ion mode. Electron energy was 70 eV and the source temperature was set at 220°C. ESI-MS analyses were performed on a LTQ XL as well as a LTQ FT Ultra (Thermo Fisher Scientific, Bremen, Germany) system. The ionization method was ESI and operated in positive ion mode. The protonated molecular ion peaks were fragmented by CID at a normalized collision energy of 35-45%. Data acquisition and analysis were accomplished with Xcalibur software version 2.0 (Thermo Fisher Scientific). HR-ESI-MS analyses were performed on a Thermo Velos Pro Orbitrap Elite (Thermo Fisher Scientific, Bremen, Germany) system. The ionization method was ESI and operated in positive ion mode. The protonated molecular ion peaks were fragmented by CID at a normalized collision energy of 35%. Data acquisition and analysis were accomplished with Xcalibur software version 2.0 (Thermo Fisher Scientific).

General procedure for the synthesis of unsubstituted benzotriazoles 5, 10-19 (Scheme 1). STEP 1. 36 mmol of 1-bromo-4-(bromomethyl)aryl derivative (**7**) was added to a solution of 6 g (50 mmol) of 1*H*-benzotriazole (**6**) in 120 mL of anhydrous tetrahydrofuran. The reaction mixture was cooled to -30°C, and a solution of 40 mL (40 mmol) of sodium-hexamethyl-disilazane (1M in THF) was added dropwise over a period of 40 min. The solution was allowed to warm up to 25°C, stirred for 2 hours, and evaporated to dryness. The residue was crystallized from an appropriate solvent to give 1-(4-bromoaryl)-1*H*-benzotriazole (**8**) in 35-40% yield. STEP 2. 28 mmol of the corresponding 1-(4-bromoaryl)-1*H*-benzotriazole (**8**) and 31 mmol of arylboronic acid (**9**) in toluene/ethanol (150 mL / 50 mL) were refluxed for 2 h with 56 mmol of Na_2CO_3 and 2.24 mmol (8 n/n%) of $Pd(PPh_3)_4$. After cooling, 180 mL of water was added and the separated organic layer was evaporated to dryness. The residue was crystallized from ethanol to give 1-(R-biaryl-4-ylmethyl)-1*H*-benzotriazoles (**5**, **10-19**) in 75-90% yield.

1-(biphenyl-4-ylmethyl)-1H-benzotriazole (5). ^{1}H NMR (400 MHz): δ 8.07 (d, *J* = 8.4 Hz, 1H, H4), 7.90 (d, *J* = 8.4 Hz, 1H, H7), 7.59-7.68 (m, 4H), 7.52-7.58 (m, 1H), 7.38-7.48 (m, 5H), 7.32-7.38 (m, 1H), 6.04 (s, 2H, CH_2N). M^+=285; EI-MS (rel. int. %): 285(68); 256(100); 180(17); 167(42); 165(20); 152(13); 128(3); 115(3); 91(4); 77(5).

1-[(2',4'-difluorobiphenyl-4-yl)methyl]-1H-benzotriazole (10). ^{1}H NMR (400 MHz): δ 8.07 (d, *J* = 8.4 Hz, 1H, H4), 7.91 (d, *J* = 8.4 Hz, 1H, H7), 7.48-7.58 (m, 4H), 7.39-7.46 (m, 3H), 7.31-7.39 (m, 1H), 7.13-7.22 (m, 1H), 6.05 (s, 2H, CH_2N). M^+=321; EI-MS (rel. int. %): 321(50); 292(100); 203(38); 201(12); 183(8); 180(10); 77(4).

1-[(4'-chloro-2'-fluorobiphenyl-4-yl)methyl]-1H-benzotriazole (11). ^{1}H NMR (800 MHz): δ 8.08 (d, *J* = 8.3 Hz, 1H, H4), 7.91 (d, *J* = 8.3 Hz, 1H, H7), 7.51-7.59 (m, 5H), 7.40-7.47 (m, 5H),

7.37 (dd, *J* = 8.8, 1.5 Hz, 1H), 6.05 (s, 2H, CH_2N). M^+=337; EI-MS (rel. int. %): 337(43); 308(100); 272(6); 219(40); 183(32); 180(15); 91(2); 77(6).

1-{[2'-fluoro-4'-(trifluoromethyl)biphenyl-4-yl]methyl}-1H-benzotriazole (12). ^{1}H NMR (400 MHz): δ 8.08 (d, *J* = 8.4 Hz, 1H, H4), 7.92 (d, *J* = 8.4 Hz, 1H, H7), 7.70-7.80 (m, 2H), 7.63-7.70 (m, 1H), 7.54-7.63 (m, 3H), 7.45-7.50 (m, 2H), 7.40-7.45 (m, 1H), 6.08 (s, 2H, CH_2N). M^+=371; EI-MS (rel. int. %): 371(35); 342(100); 253(38); 183(12); 180(10); 77(3).

1-[(2'-chloro-4'-fluorobiphenyl-4-yl)methyl]-1H-benzotriazole (13). ^{1}H NMR (400 MHz): δ 8.08 (d, *J* = 8.1 Hz, 1H, H4), 7.94 (d, *J* = 8.4 Hz, 1H, H7), 7.51-7.61 (m, 2H), 7.37-7.46 (m, 6H), 7.29 (td, *J* = 8.5, 2.7 Hz, 1H), 6.06 (s, 2H, CH_2N). M^+=337; EI-MS (rel. int. %): 337(62); 308(100); 274(20); 272(14); 219(41); 183(34); 180(18); 91(1); 77(5).

1-[(2',4'-dichlorobiphenyl-4-yl)methyl]-1H-benzotriazole (14). ^{1}H NMR (400 MHz): δ 8.08 (d, *J* = 8.4 Hz, 1H, H4), 7.94 (d, *J* = 8.4 Hz, 1H, H7), 7.71 (d, *J* = 2.0 Hz, 1H, H3"), 7.57 (t, *J* = 7.6 Hz, 1H, H6), 7.46-7.52 (m, 1H, H5"), 7.38-7.46 (m, 6H, H2', H3', H5', H6', H5, H6"), 6.06 (s, 2H, CH_2N). M^+=353; EI-MS (rel. int. %): 353(55); 324(100); 290(18); 235(40); 199(8); 180(25); 165(37); 127(7); 113(3); 77(7).

1-{[2'-chloro-4'-(trifluoromethyl)biphenyl-4-yl]methyl}-1H-benzotriazole (15). ^{1}H NMR (400 MHz): δ 8.08 (d, *J* = 8.5 Hz, 1H, H4), 7.97 (d, *J* = 0.8 Hz, 1H, H3"), 7.94 (d, *J* = 8.4 Hz, 1H, H7), 7.78 (d, *J* = 8.1 Hz, 1H, H5"), 7.54-7.65 (m, 2H, H6, H6"), 7.40-7.50 (m, 5H, H5), 6.08 (s, 2H, CH_2N). M^+=387; EI-MS (rel. int. %): 387(41); 358(100); 324(15); 269(42); 233(7); 180(19); 165(18); 77(5).

1-{[6-(4-chloro-2-fluorophenyl)pyridin-3-yl]methyl}-1H-benzotriazole (16). ^{1}H NMR (800 MHz): δ 8.80-8.83 (m, 1H, H2'), 8.07-8.10 (m, 1H, H4), 7.96-8.00 (m, 1H, H7), 7.92-7.96 (t, 1H, *J* = 8.5 Hz, H6"), 7.82-7.85 (m, 1H, H4'), 7.76-7.79 (m, 1H, H5'), 7.56-7.60 (m, 2H, H3",

H6), 7.41-7.45 (m, 2H, H5, H5"), 6.12 (s, 2H, CH_2N). M^+=338; EI-MS (rel. int. %): 338(54); 309(100); 283(10); 220(39); 193(13); 178(9); 167(12); 157(11); 77(6); 57(3).

1-{[6-(2-fluorophenyl)pyridin-3-yl]methyl}-1H-benzotriazole (17). ^{1}H NMR (400 MHz): δ 8.82 (d, *J*=2.3 Hz, 1H, H2'), 8.09 (d, *J*=8.4 Hz, 1H, H4), 7.98 (d, *J*=8.4 Hz, 1H, H7), 7.90 (dt, *J*=7.9, 1.7 Hz, 1H, H6"), 7.80-7.85 (dd, *J*=8.2, 2.3 Hz, 1H, H4'), 7.77 (dm, *J*=8.2, 7.9 Hz, 1H, H5'), 7.59 (ddd, *J*=8.4, 7.0, 0.9 Hz, 1H, H6), 7.46-7.52 (m, 1H, H4"), 7.43 (ddd, *J*=8.4, 7.0, 0.9 Hz, 1H, H5), 7.27-7.38 (m, 2H, H3", H5"), 6.12 (s, 2H, CH_2N). M^+=304; EI-MS (rel. int. %): 304(23); 275(100); 248(16); 186(21); 159(17); 133(29).

1-{[6-(4-chlorophenyl)pyridin-3-yl]methyl}-1H-benzotriazole (18). ^{1}H NMR (500 MHz)*: δ 8.76 (d, *J*=2.3 Hz, 1H, H2'), 8.07 (m, 2H, Ar", H5'), 7.93-7.99 (m, 2H, H4, H7), 7.81 (dd, *J*=8.2, 2.3 Hz, 1H, H4'), 7.77 (dm, *J*=8.2, 7.9 Hz, 1H, H5'), 7.55-7.60 (m, 1H, H6), 7.52-7.55 (m, 2H, Ar"), 7.40-7.45 (m, 1H, H5), 6.09 (s, 2H, CH2N). M^+=320; EI-MS (rel. int. %): 320(46); 291(100); 264(14); 202(34); 179(17); 149(17); 139(28); 84(46); 66(27).

1-{[5-(4-chloro-2-fluorophenyl)pyridin-2-yl]methyl}-1H-benzotriazole (19). ^{1}H NMR (400 MHz): δ 8.64-8.68 (m, 1H, H6'), 8.05-8.10 (m, 1H, H4), 8.01 (td, *J* = 8.3, 1.8 Hz, 1H, H4'), 7.83-7.88 (m, 1H, H7), 7.52-7.66 (m, 3H, H6, H3", H6"), 7.47 (d, *J* = 8.2 Hz, 1H, H3'), 7.40-7.45 (m, 2H, H5, H5"), 6.17 (s, 2H, CH_2N). M^+=338; EI-MS (rel. int. %): 310(100); 283(7); 258(7); 220(31); 207(20); 193(17); 185(21); 77(7).

General procedure for the synthesis of substituted benzotriazoles 24-60 (Scheme 2). STEP 1. A mixture of 32.5 mmol of the corresponding 1-fluoro-2-nitrobenzene (**20**), 35.8 mmol of $R^1CH_2NH_2$ (**21**) and 65 mmol of K_2CO_3 in 500 mL of AcCN was stirred for 18 h at room temperature. The solid was filtered off and washed with 30 mL of AcCN. The combined organic filtrates were evaporated in vacuo. The crude *N*-alkyl-nitrobenzenes (**22**) were obtained in 74-

90% yield and were used in the next step without further purification. STEP 2. 50 mmol of $SnCl_2$ was added to a mixture of 10 mmol of **22** in 50 mL of MeOH and 17 mL of cc. HCl and stirred at 50°C for 12 h. The mixture was concentrated in vacuo. The residue was taken up in EtOAc and washed with saturated solution of $NaHCO_3$. The combined organic layers were dried over Na_2SO_4 and concentrated in vacuo. The crude was purified by flash column chromatography on silica gel to obtain dianilines (**23**) in 52-65% yield. STEP 3. To a solution of 9.6 mmol of dianilines (**23**) in 60 mL of AcOH was added 11.6 mmol of $NaNO_2$. The mixture was stirred at 60°C for 3 h. The cooled mixture was evaporated in vacuo. The residue was taken up in EtOAc and washed with saturated solution of $NaHCO_3$. The combined organic layers were dried over Na_2SO_4 and concentrated in vacuo. The crude products were purified by flash column chromatography to give the final products **24-60** in 32-73% yield. All substituted benzotriazoles reported were prepared by the general procedure.

1-{[6-(4-chloro-2-fluorophenyl)pyridin-3-yl]methyl}-4-fluoro-1H-benzotriazole (24). ^{1}H NMR (500 MHz): δ 8.83 (dd, *J* = 2.3, 0.7 Hz, 1H, H2'), 7.95 (t, *J* = 8.6 Hz, 1H, H6"), 7.82-7.86 (m, 2H, H7, H4'), 7.77-7.80 (m, 1H, H5'), 7.56-7.61 (m, 2H, H3", H6), 7.41-7.44 (m, 1H, H5"), 7.24-7.30 (m, 1H, H5), 6.15 (s, 2H, CH_2N). ^{15}N NMR (50.7 MHz): δ -150 (N1), -65.5 (N1'), -0.5 (N2). $[M+H]^+$=357; ESI-MS-MS (rel. int. %, cid=35%): 329(100); 221(2).

1-{[6-(4-chloro-2-fluorophenyl)pyridin-3-yl]methyl}-5-fluoro-1H-benzotriazole (25). ^{1}H NMR (400 MHz): δ 8.83 (d, *J* = 1.6 Hz, 1H, H2'), 8.05 (dd, *J* = 8.9, 4.3 Hz, 1H, H7), 7.91-7.97 (m, 2H, H4, H6"), 7.81-7.87 (m, 1H, H4'), 7.75-7.81 (m, 1H, H5'), 7.50-7.60 (m, 2H, H6, H3"), 7.42 (dd, *J* = 8.5, 1.7 Hz, 1H, H5"), 6.12 (s, 2H, CH_2N). MS: $[M+H]^+$=357; ESI-MS-MS (rel. int. %, cid=35%): 329(100); 221(9).

1-{[6-(4-chloro-2-fluorophenyl)pyridin-3-yl]methyl}-6-fluoro-1H-benzotriazole (26). ^{1}H NMR (400 MHz): δ 8.83 (d, *J* = 1.6 Hz, 1H, H2'), 8.15 (dd, *J* = 9.1, 4.7 Hz, 1H, H4), 7.92-7.97 (m, 2H, H7, H6"), 7.83-7.89 (m, 1H, H4'), 7.75-7.81 (m, 1H, H5'), 7.58 (dd, *J* = 11.2, 2.0 Hz, 1H, H3"), 7.42 (dd, *J* = 8.5, 2.0 Hz, 1H, H5"), 7.34 (dt, *J* = 9.1, 2.3, Hz, 1H, H5), 6.07 (s, 2H, CH_2N). $[M+H]^+$=357; ESI-MS-MS (rel. int. %, cid=35%): 329(100); 221(19).

1-{[6-(4-chloro-2-fluorophenyl)pyridin-3-yl]methyl}-1H-benzotriazole-4-carbonitrile (27). ^{1}H NMR (400 MHz): δ 8.83-8.85 (m, 1H, H2'), 8.41 (dd, *J* = 8.5, 0.7 Hz, 1H, H7), 8.06 (dd, *J* = 7.2, 0.7 Hz, 1H, H5), 7.94 (t, *J* = 8.6 Hz, 1H, H6"), 7.83-7.88 (m, 1H, H4'), 7.74-7.80 (m, 2H, H6, H5'), 7.57 (dd, *J* = 11.2, 2.0 Hz, 1H, H3"), 7.42 (dd, *J* = 8.5, 1.6 Hz, 1H, H5"), 6.20 (s, 2H, CH_2N). $[M+H]^+$=364; ESI-MS-MS (rel. int. %, cid=35%): 336(100); 221(9).

1-{[6-(4-chloro-2-fluorophenyl)pyridin-3-yl]methyl}-4-(trifluoromethyl)-1H-benzotriazole (28). ^{1}H NMR (800 MHz): δ 8.85-8.88 (m, 1H, H2'), 8.37 (d, *J* = 8.3 Hz, 1H, H7), 7.95 (t, *J* = 8.7 Hz, 1H, H6"), 7.84-7.88 (m, 2H, H5, H4'), 7.75-7.81 (m, 2H, H5', H6), 7.58 (dd, *J* = 11.2, 2.0 Hz, 1H, H3"), 7.43 (dd, *J* = 8.3, 2.0 Hz, 1H, H5"), 6.21 (s, 2H, CH_2N). ^{13}C NMR (201 MHz): δ 159.6 (d, $^{1}J_F$ = 253 Hz, C2"), 151.3 (d, $^{3}J_F$ = 2.4 Hz, C6'), 149.4 (C2'), 140.7 (C3a), 136.7 (C4'), 134.5 (d, $^{3}J_F$ = 10.3 Hz, C4"), 133.7 (C7a), 132.0 (d, $^{3}J_F$ = 4.0 Hz, C6"), 130.5 (C3'), 127.3 (C6), 125.4 (d, $^{2}J_F$ = 11.9 Hz, C1"), 125.2 (d, $^{4}J_F$ = 3.2 Hz, C5"), 124.1 (d, $^{4}J_F$ = 9.5 Hz, C5'), 123.3 (q, $^{1}J_F$ = 272 Hz, CF_3), 122.2 (q, $^{3}J_F$ = 4.8 Hz, C5), 119.3 (q, $^{2}J_F$ = 33.5 Hz, C4), 116.9 (d, $^{2}J_F$ = 27.0 Hz, C3"), 115.9 (C7), 48.5 (CH_2N). ^{15}N NMR (81.1 MHz): δ -149 (N1), -65 (N1'), 1.6 (N2). $[M+H]^+$=407; ESI-MS-MS (rel. int. %, cid=35%): 379(100); 359(16); 339(3); 221(7).

1-{[6-(4-chloro-2-fluorophenyl)pyridin-3-yl]methyl}-4-bromo-1H-benzotriazole (29). ^{1}H NMR (800 MHz): δ 8.83 (d, *J* = 1.6 Hz, 1H, H2'), 8.01 (d, *J* = 8.3 Hz, 1H, H7), 7.95 (t, *J* = 8.5

Hz, 1H, H6"), 7.82-7.85 (m, 1H, H4'), 7.76-7.79 (m, 1H, H5'), 7.70 (d, J = 6.7 Hz, 1H, H5), 7.58 (dd, J = 11.0, 2.0 Hz, 1H, H3"), 7.52 (dd, J = 8.3, 7.5 Hz, 1H, H6), 7.42 (dd, J = 8.7, 2.0 Hz, 1H, H5"), 6.13 (s, 2H, CH_2N). ^{13}C NMR (201 MHz): δ 159.6 (d, ^1J_F = 252 Hz, C2"), 151.3 (d, ^3J_F = 2.4 Hz, C6'), 149.3 (C2'), 144.0 (C3a), 136.6 (C4'), 134.5 (d, ^3J_F = 10.7 Hz, C4"), 133.8 (C7a), 132.0 (d, ^3J_F = 3.6 Hz, C6"), 130.6 (C3'), 129.0 (C6), 127.2 (C5), 125.4 (d, ^2J_F = 11.9 Hz, C1"), 125.2 (d, ^4J_F = 3.6 Hz, C5"), 124.1 (d, ^4J_F = 8.7 Hz, C5'), 116.9 (d, ^2J_F = 27.0 Hz, C3"), 111.8 (C4), 110.4 (C7), 48.7 (CH_2N). ^{15}N NMR (81.1 MHz): δ -149 (N1), -65 (N1'), -0.5 (N2). $[M+H]^+$=417; ESI-MS-MS (rel. int. %, cid=35%): 389(95); 310(15); 221(10).

1-benzyl-4-bromo-1H-benzotriazole (30). ^1H NMR (400 MHz): δ 7.88 (d, J = 8.3 Hz, 1H, H7), 7.66 (d, J = 7.4 Hz, 1H, H5), 7.48 (dd, J = 8.3, 7.4 Hz, 1H, H6), 7.27-7.41 (m, 5H), 6.01 (s, 2H, CH_2N). M^+=287; EI-MS (rel. int. %): 287(78); 258(61); 180(59); 152(15); 104(5); 91(100); 76(8); 65(18).

4-bromo-1-(2-fluorobenzyl)-1H-benzotriazole (31). ^1H NMR (400 MHz): δ 7.87 (d, J = 8.3 Hz, 1H, H7), 7.68 (d, J = 7.4 Hz, 1H, H5), 7.49 (dd, J = 8.3, 7.4 Hz, 1H, H6), 7.36-7.44 (m, 2H), 7.19-7.27 (m, 2H), 6.06 (s, 2H, CH_2N). M^+=305; EI-MS (rel. int. %): 305(55); 276(40); 258(8); 198(28); 170(7); 155(3); 109(100).

4-bromo-1-(3-fluorobenzyl)-1H-benzotriazole (32). ^1H NMR (400 MHz): δ 7.91 (dd, J = 8.3, 0.7 Hz, 1H, H7), 7.68 (dd, J = 7.5, 0.7 Hz, 1H, H5), 7.49 (dd, J = 8.3, 7.5 Hz, 1H, H6), 7.36-7.45 (m, 1H), 7.11-7.25 (m, 3H), 6.04 (s, 2H, CH_2N). M^+=305; EI-MS (rel. int. %): 305(61); 276(35); 258(6); 198(51); 170(11); 155(4); 109(100).

4-bromo-1-(4-fluorobenzyl)-1H-benzotriazole (33). ^1H NMR (400 MHz): δ 7.91 (d, J = 8.1 Hz, 1H, H7), 7.68 (d, J = 7.5 Hz, 1H, H5), 7.49 (dd, J = 8.3, 7.5 Hz, 1H, H6), 7.39-7.45 (m, 2H,

H2', H6'), 7.15-7.23 (m, 2H, H3', H5'), 6.00 (s, 2H, CH_2N). M^+=305; EI-MS (rel. int. %): 305(68); 276(49); 258(4); 198(45); 170(12); 155(3); 109(100).

4-bromo-1-(4-chlorobenzyl)-1H-benzotriazole (34). ^{1}H NMR (400 MHz): δ 7.89 (dd, *J* = 8.3, 0.7 Hz, 1H, H7), 7.68 (dd, *J* = 7.5, 0.7 Hz, 1H, H5), 7.48 (dd, *J* = 8.3, 7.5 Hz, 1H, H6), 7.40-7.45 (m, 2H, H2', H6'), 7.33-7.39 (m, 2H, H3', H5'), 6.01 (s, 2H, CH_2N). M^+=321; EI-MS (rel. int. %): 321(74); 292(25); 258(55); 214(21); 179(46); 155(4); 125(100); 89(30).

4-bromo-1-(4-bromobenzyl)-1H-benzotriazole (35). ^{1}H NMR (400 MHz): δ 7.89 (d, *J* = 8.4 Hz, 1H, H7), 7.68 (d, *J* = 7.5 Hz, 1H, H5), 7.54-7.58 (m, 2H, H3', H5'), 7.48 (dd, *J* = 8.4, 7.5 Hz, 1H, H6), 7.27-7.31 (m, 2H, H2', H6'), 6.00 (s, 2H, CH_2N). $[M+H]^+$=366; ESI-MS-MS (rel. int. %, cid=35%): 338(1); 258(2); 169(100).

4-bromo-1-(2-chloro-4-fluorobenzyl)-1H-benzotriazole (36). ^{1}H NMR (400 MHz): δ 7.85 (d, *J* = 8.3 Hz, 1H, H7), 7.69 (d, *J* = 7.4 Hz, 1H, H5), 7.55 (dd, *J* = 8.9, 2.5 Hz, 1H, H3'), 7.49 (dd, *J* = 8.3, 7.4 Hz, 1H, H6), 7.40 (dd, *J* = 8.6, 6.2 Hz, 1H, H6'), 7.26 (td, *J* = 8.5, 2.5 Hz, 1H, H5'), 6.06 (s, 2H, CH_2N). M^+=339; EI-MS (rel. int. %): 339(28); 310(21); 292(2); 276(30); 232(13); 197(34); 170(8); 155(4); 143(100); 107(19).

4-bromo-1-(4-chloro-3-fluorobenzyl)-1H-benzotriazole (37). ^{1}H NMR (400 MHz): δ 7.92 (dd, *J* = 8.4, 0.6 Hz, 1H, H7), 7.69 (dd, *J* = 7.4, 0.6 Hz, 1H, H5), 7.58 (t, *J* = 8.1 Hz, 1H, H5'), 7.45-7.52 (m, 2H, H6, H2'), 7.12-7.17 (m, 1H, H6'), 6.03 (s, 2H, CH_2N). M^+=339; EI-MS (rel. int. %): 339(61); 310(19); 292(4); 276(28); 232(37); 197(24); 170(7); 155(5); 143(100); 107(18).

4-bromo-1-(4-chloro-2-fluorobenzyl)-1H-benzotriazole (38). ^{1}H NMR (400 MHz): δ 7.89 (d, *J* = 8.6 Hz, 1H, H7), 7.69 (d, *J* = 7.4 Hz, 1H, H5), 7.48-7.53 (m, 2H, H6, H3'), 7.42 (t, *J* = 8.2 Hz, 1H, H6'), 7.31 (dd, *J* = 8.2, 1.8 Hz, 1H, H5'), 6.05 (s, 2H, CH_2N). $[M+H]^+$=340; ESI-MS-MS (rel. int. %, cid=35%): 312(4); 276(2); 233(4); 143(100).

4-bromo-1-[(5-bromopyridin-2-yl)methyl]-1H-benzotriazole (39). ^{1}H NMR (400 MHz): δ 8.57-8.61 (m, 1H, H6'), 8.06-8.12 (m, 1H, H4'), 7.83 (d, *J* = 8.3 Hz, 1H, H7), 7.68 (d, *J* = 7.5 Hz, 1H, H5), 7.47 (dd, *J* = 8.3, 7.5 Hz, 1H, H6), 7.38-7.43 (m, 1H, H3'), 6.12 (s, 2H, CH_2N). M^+=366; EI-MS (rel. int. %): 366(1); 338(49); 259(46); 170(48); 143(17); 90(31).

4-bromo-1-[(6-bromopyridin-3-yl)methyl]-1H-benzotriazole (40). ^{1}H NMR (400 MHz): δ 8.51-8.54 (m, 1H, H2'), 7.96 (dd, *J* = 8.3, 0.7 Hz, 1H, H7), 7.61-7.72 (m, 3H, H5, H4', H5'), 7.50 (dd, *J* = 8.3, 7.5 Hz, 1H, H6), 6.05 (s, 2H, CH_2N). M^+=366; EI-MS (rel. int. %): 366(1); 337(16); 259(46); 170(54); 143(11); 90(29).

4-bromo-1-[(6-chloropyridin-3-yl)methyl]-1H-benzotriazole (41). ^{1}H NMR (400 MHz): δ 8.55 (d, *J* = 2.5 Hz, 1H, H2'), 7.96 (d, *J* = 8.4 Hz, 1H, H7), 7.78 (dd, *J* = 8.3, 2.5 Hz, 1H, H4'), 7.69 (dd, *J* = 7.4, 0.6 Hz, 1H, H5), 7.47-7.54 (m, 2H, H6, H5'), 6.07 (s, 2H, CH_2N). M^+=322; EI-MS (rel. int. %): 322(55); 293(35); 259(29); 215(32); 179(41); 126(100).

4-bromo-1-(cyclohexylmethyl)-1H-benzotriazole (42). ^{1}H NMR (500 MHz): δ 7.94 (d, *J* = 8.3 Hz, 1H, H7), 7.66 (d, *J* = 7.3 Hz, 1H, H5), 7.48 (dd, *J* = 8.3, 7.3 Hz, 1H, H6), 4.58 (d, *J* = 7.3 Hz, 2H, CH_2N), 1.90-2.00 (m, 1H, CH), 1.46-1.69 (m, 5H, 5xCH_2eq), 0.97-1.22 (m, 5H, 5xCH_2ax). ^{15}N NMR (50.7 MHz): δ -160 (N1), -11 (N2). M^+=293; EI-MS (rel. int. %): 293(43); 210(100); 197(11); 182(54); 169(4); 155(19); 130(4); 117(3); 103(22); 83(21); 75(14); 55(58); 41(31).

4-bromo-1-(cyclopentylmethyl)-1H-benzotriazole (43). ^{1}H NMR (400 MHz): δ 7.97 (d, *J* = 8.3 Hz, 1H, H7), 7.66 (d, *J* = 7.4 Hz, 1H, H5), 7.48 (dd, *J* = 8.3, 7.4 Hz, 1H, H6), 4.66 (d, *J* = 7.4 Hz, 2H, CH_2N), 2.44-2.55 (m, 1H, CH), 1.47-1.67 (m, 6H), 1.23-1.34 (m, 2H). M^+=279; EI-MS (rel. int. %): 279(38); 210(100); 182(53); 169(7); 155(18); 130(5); 103(20); 90(5); 75(15); 69(21); 55(17); 41(39).

4-bromo-1-(cyclobutylmethyl)-1H-benzotriazole (44). ^{1}H NMR (500 MHz): δ 7.96 (d, *J* = 7.8 Hz, 1H, H7), 7.66 (d, *J* = 6.9 Hz, 1H, H5), 7.46-7.50 (m, 1H, H6), 4.76 (d, *J* = 7.3 Hz, 2H, CH_2N), 2.86-2.96 (m, 1H, CH), 1.78-2.01 (m, 6H, 3xcybCH_2). ^{15}N NMR (50.7 MHz): δ -160 (N1), -13 (N2). M^+=265; EI-MS (rel. int. %): 265(82); 237(19); 224(19); 210(99); 197(8); 182(44); 169(20); 155(25); 130(40); 117(22); 103(30); 90(16); 75(29); 55(100); 41(68).

4-bromo-1-(cyclopropylmethyl)-1H-benzotriazole (45). ^{1}H NMR (400 MHz): δ 7.99 (dd, *J* = 8.3, 0.6 Hz, 1H, H7), 7.67 (dd, *J* = 7.4, 0.6 Hz, 1H, H5), 7.49 (dd, *J* = 8.3, 7.4 Hz, 1H, H6), 4.63 (d, *J* = 7.3 Hz, 2H, CH_2N), 1.33-1.43 (m, 1H, CH), 0.51-0.58 (m, 2H, cypCH_2x), 0.46-0.51 (m, 2H, cypCH_2y). M^+=251; EI-MS (rel. int. %): 251(64); 222(25); 210(59); 195(13); 182(30); 169(14); 155(22); 143(41); 116(35); 75(27); 55(100).

4-bromo-1-(2-methylpropyl)-1H-benzotriazole (46). ^{1}H NMR (400 MHz): δ 7.95 (d, *J* = 8.4 Hz, 1H, H7), 7.67 (d, *J* = 7.4 Hz, 1H, H5), 7.48 (dd, *J* = 8.3, 7.4 Hz, 1H, H6), 4.56 (d, *J* = 7.0 Hz, 2H, CH_2N), 2.28 (n, *J* = 7.0 Hz, 1H, CH), 0.89 (d, *J* = 7.0 Hz, 6H, 2xCH_3). M^+=253; EI-MS (rel. int. %): 253(48); 210(100); 182(52); 169(13); 155(21); 130(6); 117(2); 103(22); 90(6); 75(16); 43(13); 41(14).

4-bromo-1-butyl-1H-benzotriazole (47). ^{1}H NMR (500 MHz)*: δ 7.94 (dd, *J* = 8.3, 0.6 Hz, 1H, H7), 7.67 (dd, *J* = 7.4, 0.6 Hz, 1H, H5), 7.48 (dd, *J* = 8.3, 7.4 Hz, 1H, H6), 4.73 (t, *J*=7.0 Hz, 2H, CH_2N), 1.84-1.94 (m, 2H, $CH_2$2'), 1.21-1.30 (m, 2H, $CH_2$3'), 0.89 (t, *J*=7.4 Hz, 3H, CH_3). HRMS: $[M+H]^+$=254.02877 ($C_{10}H_{13}N_3Br$; delta=0.13); ESI-MS-MS (rel. int. %, cid=45%): 198(100).

4-bromo-1-propyl-1H-benzotriazole (48). ^{1}H NMR (800 MHz): δ 7.95 (d, *J* = 8.2 Hz, 1H, H7), 7.67 (d, *J* = 7.4 Hz, 1H, H5), 7.49 (dd, *J* = 8.3, 7.4 Hz, 1H, H6), 4.70 (t, *J* = 7.0 Hz, 2H, CH_2N), 1.94 (sx, *J* = 7.4 Hz, 2H, CH_2), 0.85 (t, *J* = 7.4 Hz, 3H, CH_3). M^+=239; EI-MS (rel. int.

%): 239(100); 210(57); 182(50); 169(89); 155(33); 117(17); 103(25); 90(34); 75(29); 43(22); 41(23).

4-bromo-1-ethyl-1H-benzotriazole (49). ^{1}H NMR (500 MHz)*: δ 7.94 (dd, *J* = 8.3, 0.6 Hz, 1H, H7), 7.67 (dd, *J* = 7.4, 0.6 Hz, 1H, H5), 7.48 (dd, *J* = 8.3, 7.4 Hz, 1H, H6), 4.76 (q, *J* = 7.3 Hz, 2H, CH_2), 1.52 (t, *J* = 7.3 Hz, 3H, CH_3). HRMS: $[M+H]^+$=225.99756 ($C_8H_9N_3Br$; delta=0.55); ESI-MS-MS (rel. int. %, cid=45%): 198(100).

4-bromo-1-methyl-1H-benzotriazole (50). ^{1}H NMR (800 MHz): δ 7.89 (d, *J* = 8.4 Hz, 1H, H7), 7.67 (d, *J* = 7.4 Hz, 1H, H5), 7.46-7.52 (m, 1H, H6), 4.33 (s, 3H, CH_3N). M^+=211; EI-MS (rel. int. %): 211(93); 183(100); 168(65); 155(14); 117(6); 104(23); 88(15); 77(43); 63(29); 51(21).

4-bromo-1-(cyclopropylmethyl)-6-(trifluoromethyl)-1H-benzotriazole (51). ^{1}H NMR (500 MHz): δ 8.61-8.64 (m, 1H, H7), 8.02 (d, *J* = 0.9 Hz, 1H, H5), 4.74 (d, *J* = 7.4 Hz, 2H, CH_2N), 1.40-1.49 (m, 1H, CH), 0.53-0.58 (m, 2H, cypCH_2x), 0.48-0.53 (m, 2H, cypCH_2y). M^+=319; EI-MS (rel. int. %): 319(39); 290(13); 278(100); 250(33); 221(23); 184(18); 144(18); 55(65).

4,6-dibromo-1-(cyclopropylmethyl)-1H-benzotriazole (52). ^{1}H NMR (500 MHz): δ 8.39 (d, *J* = 1.4 Hz, 1H, H7), 7.88 (d, *J* = 1.4 Hz, 1H, H5), 4.61 (d, *J* = 7.3 Hz, 2H, CH_2N), 1.35-1.43 (m, 1H, CH), 0.51-0.58 (m, 2H, cypCH_2x), 0.44-0.50 (m, 2H, cypCH_2y). M^+=329; EI-MS (rel. int. %): 329(34); 288(45); 260(15); 221(13); 143(15); 115(18); 55(90).

4-bromo-6-chloro-1-(cyclopropylmethyl)-1H-benzotriazole (53). ^{1}H NMR (800 MHz): δ 8.25 (d, *J* = 1.6 Hz, 1H, H7), 7.79 (d, *J* = 1.6 Hz, 1H, H5), 4.61 (d, *J* = 7.4 Hz, 2H, CH_2N), 1.37-1.45 (m, 1H, cyp-CHalpha), 0.51-0.58 (m, 2H, cyp-CH_2alpha), 0.45-0.51 (m, 2H, cyp-CH_2beta). ^{13}C{1H} NMR (201 MHz): δ 142.9 (C3a), 133.9 (7a), 132.5 (C6), 126.9 (C5), 112.6 (C4), 110.5

(C7), 52.5 (CH_2N), 11.1 (cyp-CH), 3.9 (cyp-CH_2). ^{15}N NMR (81.1 MHz): δ -144 (N1), 2 (N2). M^+=285; EI-MS (rel. int. %): 285(50); 244(79); 216(25); 177(21); 55(95).

4-bromo-6-fluoro-1-(cyclopropylmethyl)-1H-benzotriazole **(54).** ^1H NMR (500 MHz): δ 7.94 (dd, *J*= 8.5, 2.1 Hz, 1H, H7), 7.72 (dd, *J* = 9.0, 2.1 Hz, 1H, H5), 4.58 (d, *J* = 7.3 Hz, 2H, CH_2N), 1.33-1.43 (m, 1H, CH), 0.52-0.58 (m, 2H, cypCH_2x), 0.46-0.51 (m, 2H, cypCH_2y). M^+=269; EI-MS (rel. int. %): 269(46); 241(10); 228(100); 200(25); 187(11); 173(17); 161(29); 134(27); 121(26); 107(19); 94(23); 55(62).

4-bromo-1-(cyclopropylmethyl)-6-methoxy-1H-benzotriazole (55). 1H NMR (500 MHz): δ 7.42 (d, J = 2.0 Hz, 1H, H7), 7.31 (d, J = 2.0 Hz, 1H, H5), 4.55 (d, J = 7.2 Hz, 2H, CH2N), 1.33-1.45 (m, 1H, CH), 0.51-0.58 (m, 2H, cypCH2x), 0.43-0.50 (m, 2H, cypCH2y). M^+=281; EI-MS (rel. int. %): 281(100); 252(11); 240(56); 212(46); 199(14); 184(17); 173(11); 159(14); 146(9); 133(18); 104(14); 90(12); 76(15); 63(15); 55(99).

4-chloro-1-(cyclopropylmethyl)-1H-benzotriazole (56). 1H NMR (500 MHz): δ 7.95 (dd, J = 8.0, 1.0 Hz, 1H, H7), 7.55 (t, J = 7.5 Hz, 1H, H6), 7.52 (dd, J = 7.3, 1.0 Hz, 1H, H5), 4.65 (d, J = 7.3 Hz, 2H, CH2N), 1.32-1.44 (m, 1H, CH), 0.52-0.61 (m, 2H, cypCH2x), 0.42-0.51 (m, 2H, cypCH2y). M^+=207; EI-MS (rel. int. %): 207(100); 178(43); 166(93); 151(28); 143(30); 138(52); 125(26); 111(45); 102(14); 89(17); 75(32); 63(11); 51(91).

4-fluoro-1-(cyclopropylmethyl)-1H-benzotriazole (57). ^1H NMR (800 MHz): δ 7.80 (d, *J* = 8.4 Hz, 1H, H7), 7.56 (td, *J* = 8.0, 4.6 Hz, 1H, H6), 7.24 (dd, *J* = 10.8, 7.7 Hz, 1H, H5), 4.64 (d, *J* = 7.3 Hz, 2H, CH_2N), 1.33-1.44 (m, 1H, CH), 0.55-0.58 (m, 2H, cypCH_2x), 0.47-0.50 (m, 2H, cypCH_2y). $^{13}C\{1H\}$ NMR (201 MHz): δ 152.2 d ^1J_F = 255 Hz (C4), 135.8 d ^3J_F = 6.8 Hz (7a), 135.1 d ^2J_F = 18.7 Hz (C3a), 128.2 d ^3J_F = 7.2 Hz (C6), 108.3 d ^2J_F = 16.8 Hz (C5), 107.4 d ^4J_F = 4.8 Hz (C7), 52.3 (CH_2N), 11.1 (cyp-CH), 3.9 (cyp-CH_2). ^{15}N NMR (81.1 MHz): δ -145 (N1), 0

(N2). M^+=191; EI-MS (rel. int. %): 191(69); 162(25); 150(100); 135(23); 122(41); 108(26); 95(52); 75(15); 55(39).

1-(cyclopropylmethyl)-1H-benzotriazole-4-carbonitrile (58). ^{1}H NMR (400 MHz): δ 8.40 (d, *J* = 8.5 Hz, 1H, H7), 8.04 (d, *J* = 7.2, 1H, H5), 7.74 (dd, *J* = 8.5, 7.2 Hz, 1H, H6), 4.71 (d, *J* = 7.3 Hz, 2H, CH_2N), 1.34-1.46 (m, 1H, CH), 0.53-0.61 (m, 2H, cypCH_2x), 0.45-0.53 (m, 2H, cypCH_2y). M^+=198; EI-MS (rel. int. %): 198(29); 169(25); 157(100); 149(10); 142(19); 129(38); 116(18); 102(28); 75(8); 55(37).

1-(cyclopropylmethyl)-4-methoxy-1H-benzotriazole (59). ^{1}H NMR (500 MHz)*: δ 7.40-7.46 (m, 2H, H6, H7), 6.81 (dd, *J* = 6.9, 1.5 Hz, 1H, H5), 4.55 (d, *J* = 7.2 Hz, 2H, CH_2N), 4.02 (s, 3H, OMe), 0.82-0.88 (m, 1H, CH), 0.51-0.57 (m, 2H, cypCH_2x), 0.42-0.47 (m, 2H, cypCH_2y). M^+=203; EI-MS (rel. int. %): 203(100); 202(67); 189(29); 174(72); 163(50); 151(52); 145(32); 121(31); 117(40); 91(42); 66(80).

1-(cyclopropylmethyl)-4-(trifluoromethyl)-1H-benzotriazole (60). ^{1}H NMR (800 MHz): δ 8.33 (d, *J* = 8.4 Hz, 1H, H7), 7.82 (d, *J* = 7.2 Hz, 1H, H5), 7.72-7.75 (m, 1H, H6), 4.71 (d, *J* = 7.3 Hz, 2H, CH_2N), 1.38-1.44 (m, 1H, CH), 0.54-0.58 (m, 2H, cypCH_2x), 0.49-0.53 (m, 2H, cypCH_2y). ^{13}C{1H} NMR (100.5 MHz): δ 140.5 (C3a), 133.7 (7a), 126.7 (C6), 121.9 (q, $^3J_{CF}$=5 Hz, C5), 123.1 (q, $^1J_{CF}$=272 Hz, CF3), 119.0 (q, $^2J_{CF}$=33.5 Hz, C4), 116.0 (C7), 52.3 (CH_2N), 11.2 (cyp-CH), 3.9 (cyp-CH_2). HRMS: $[M+H]^+$=242.08966 ($C_{11}H_{11}N_3F_3$; delta=-1.2); ESI-MS-MS (rel. int. %, cid=35%): 240(2); 222(6); 188(100); 168(3).

Biological evaluation. Human mGluR2 in vitro functional assay. Chem-1 cells stably expressing human mGlu2 receptors were cultured in the medium detailed above. Fluorometric measurements of cytosolic Ca^{2+} ion concentration ($[Ca^{2+}]_i$) were carried out using cells seeded in standard 96-well microplates at a density of 30000 cells/well and maintained overnight in a tissue culture incubator at 37 °C under an atmosphere of 95 % air/5 % CO_2. Composition of the plating medium was: DMEM, 10 % FBS, 1× MEM non-essential amino acids (Sigma M 7145), 1× PSA. The growth medium was removed and the cells were washed with assay buffer (without GPT/pyruvate), both actions were performed with a cell washer (BioTek Elx405UCVWS). At the end of the washing step 50 µl/well assay buffer (without GPT/pyruvate) was left in the wells, and 50 µl/well Calcium 5 kit diluted 4-fold in assay buffer (with 6 µg/ml GPT/4 mM pyruvate) was added manually using an 8-channel pipette. After an incubation period (30 min, 37 °C) the dye was removed and the cells were washed with the cell washer using the same protocol as above. After washing the plate was incubated for 10 min at 37 °C. Then 50 µl/well assay buffer (with 6 µg/ml GPT/4 mM pyruvate) containing vehicle (DMSO) or the test compounds or reference mGluR2 positive modulators was added manually and the cells were incubated for an additional 30 min at 37 °C. Baseline and agonist-evoked $[Ca^{2+}]_i$-changes were monitored with FlexStation II (Molecular Devices, Sunnyvale, CA), a plate reader fluorometer with integrated 8-channel fluid addition capability. Fluorescence measurements were carried out at 37 °C. The dye was excited at 485 nm, emission was sampled at 525 nm at 1.4-s intervals. Baseline was recorded for 20 s followed by agonist stimulation. The 50 µl 3× concentrated agonist solution was added to the cells using the pipettor of FlexStation II and fluorescence was monitored for an additional 40 s. Agonist was glutamate administered at an EC_5-EC_{20} concentration. Final DMSO concentration was 1 % for all treatments. To achieve this a series of DMSO stock solutions were

prepared from all test compounds. These stocks were stored under 0 °C and were further diluted in assay buffer without GPT/pyruvate to obtain the desired final concentration immediately before the measurement. Results were expressed as ΔF/F values using SoftMax Pro software (Molecular Devices), where F was the resting fluorescence preceding agonist application and ΔF was the increase in fluorescence at a given time (ΔF = maximum fluorescence intensity values after stimulation minus average fluorescence intensity values before stimulation). In all experiments, all treatments were measured in multiple wells in parallel, and the mean ΔF/F values were used for analysis. Where appropiate, sigmoid curves were fitted to the concentration–response data to obtain EC_{50} values.

Human, rat and mouse liver microsomal stability assay. In vitro metabolic stability was assessed using human (Xenotech, USA), Wistar rat (In Vitro Metabolism Research, Gedeon Richter Plc, Hungary) and NMRI mice (In Vitro Metabolism Research, Gedeon Richter Plc, Hungary) liver microsomes. Test compounds at 2.5 μM initial test concentration were incubated for various lengths of time with the liver microsomes (0.5 mg/mL). In vitro intrinsic clearance (Cl_{int} mL/min·g liver) was calculated using the basic concept of clearance prediction34 according to the following equations: $Cl_{int} = V_{max}/K_M$ or, if $S \ll K_M$, $Cl_{int} = V/S$; V_{max} = maximal rate of enzyme reaction; K_M = affinity constant of substrate concentration; V = actual rate of enzyme reaction under first order conditions.

Animals. Male mice of ddY strains (6 weeks old) were purchased from Japan SLC (Shizuoka, Japan). All animal experiments were performed under experimental protocols approved by the Institutional Animal Care and Use Committee, Mitsubishi Tanabe Pharma Corporation.

PCP-induced hyperlocomotion. Locomotor activity was measured using the passive infrared sensor system (Supermex®; Muromachi Kikai, Japan). Mice acclimated to the test cage for 60

min, and were injected intraperitoneally with the test compounds. Immediately, mice were injected with PCP (2.5 mg/kg, s.c.), then were placed back in the test cage for another 60 min, during which locomotor activity was recorded.

DOI-induced head twitches. The test compounds were injected intraperitoneally 20 min prior to injection of DOI (0.75 mg/kg, s.c.). The number of head twitches were counted in a transparent cylinder (height: 25.5 cm, diameter: 19 cm) for the period between 10 and 18 min (8 min) after the DOI injection.

ANCILLARY INFORMATION

Supporting Information

Molecular Formula Strings

Corresponding author information

*(Gy.Sz.) Phone: +36-1-4315180 E-mail: gy.szabo@richter.hu

*(G.M.K) Phone: +36-1-3826821 E-mail: gy.keseru@mta.ttk.hu

Author Contributions

The manuscript was written through contributions of all authors. All authors have given approval to the final version of the manuscript.

Abbreviations used

AcOH, acetic acid; AcCN, acetonitrile; ADME, absorption, distribution, metabolism, excretion; Cl_{int}, intrinsic clearance; C_{plasma}, plasma concentrations; $C_{plasma\ unbound}$, unbound plasma concentrations; C_{brain}, brain concentrations; DMF, *N,N*-dimethylformamide; DOI, 2,5-dimethoxy-4-iodoamphetamine; EtOAc, ethyl acetate; FBDD, fragment based drug discovery; GE, group efficiency; GPCR, Gprotein-coupled receptor; h, hours; HTS, high-throughput screening; LE, ligand efficiency; mGlu2, metabotropic glutamate 2; MeOH, methanol; MW, molecular weight; NaHMDS, sodium bis(trimethylsilyl)amide; ND, not determined; NMR, nuclear magnetic resonance; PAM, positive allosteric modulator; PANSS, positive and negative syndrome scale; PCP, phencyclidine; PK, pharmacokinetics; SAR, structure−activity relationship; SEM, standard error of mean; HPLC, high-performance liquid chromatography; SD, standard deviation; THF, tetrahydrofuran; TPSA, topological polar surface area

REFERENCES AND NOTES

(1) Niswender, C. M.; Conn, P. J. Metabotropic Glutamate Receptors: Physiology, Pharmacology, and Disease. *Ann. Rev. Pharmacol. Toxicol.*. **2010**, *50*, 295–322.

(2) Petralia, R. S.; Wang, Y. X.; Niedzielski, A. S.; Wenthold, R. J. The metabotropic glutamate receptors, mGluR2 and mGluR3, show unique postsynaptic, presynaptic and glial localizations, *Neuroscience*, **1996**, *71*, 949–976.

(3) Anwyl, R. Metabotropic glutamate receptors: electrophysiological properties and role in plasticity. *Brain Res. Rev.* **1999**, *29*, 83–120.

(4) Moreno, J. L.; Sealfon, S. C.; Gonzalez-Maeso, J. Group II metabotropic glutamate receptors and schizophrenia. *Cell Mol. Life Sci.* **2009***, 66***,** 3777–3785.

(5) Chaki, S. Group II metabotropic glutamate receptor agonists as a potential drug for schizophrenia. *Eur. J. Pharmacol.* **2010**, *639***,** 59–66.

(6) Fell, M. J.; Svensson, K. A.; Johnson, B. G.; Schoepp, D. D. Evidence for the role of metabotropic glutamate mGlu2 not mGlu3 receptors in the preclinical antipsychotic pharmacology of the mGlu2/3 receptor agonist (-)-(1R,4S,5S,6S)-4-amino-2-sulfonylbicyclo[3.1.0]hexane-4,6-dicarboxylic acid (LY404039). *J. Pharmacol. Exp. Ther.* **2008**, *326***,** 209–217

(7) Reznik, A. M.; Smulevich, A. B.; Tochilov, V. A.; Johnson, B. G.; Monn, J. A.; Schoepp, D. D. Activation of mGlu2/3 receptors as a new approach to treat schizophrenia: a randomized Phase 2 clinical trial. *Nat. Med*. **2007**, *13***,** 1102–1107.

(8) Adams, D. H.; Kinon, B. J.; Baygani, S.; Millen, B. A.; Velona, I.; Kollack-Walker, S.; Walling, D. P. A long-term, phase 2, multicenter, randomized, open-label, comparative safety study of pomaglumetad methionil (LY2140023 monohydrate) versus atypical antipsychotic standard of care in patients with schizophrenia. *BMC. Psychiatry* **2013**, *13***,** 143.

(9) Adams, D. H.; Zhang, L.; Millen, B. A.; Kinon, B. J.; Gomez, J. C. Pomaglumetad methionil (LY2140023 monohydrate) and aripiprazole in patients with schizophrenia: a phase 3, multicenter, double-blind comparison. *Schizophr. Res. Treat.* **2014**, 758212.

(10) Rowe, B. A.; Schaffhauser, H.; Morales, S.; Lubbers, L. S.; Bonnefous, C.; Kamenecka, T. M.; McQuiston, J.; Daggett, L. P. Transposition of three amino acids transforms the human metabotropic glutamate receptor (mGluR)-3-positive allosteric modulation site to mGluR2, and additional characterization of the mGluR2-positive allosteric modulation site. *J. Pharmacol. Exp. Ther.* **2008**, *326*, 240–251.

(11) Rudd, M. T.; McCauley, J. A. Positive allosteric modulators of the metabotropic glutamate receptor subtype 2 (mGluR2). *Curr. Top. Med. Chem*. **2005**, *5*, 869–884.

(12) Szabó, G.; Keserű, G. M. Positive allosteric modulators for mGluR2 receptors: a medicinal chemistry perspective. *Curr. Top. Med. Chem.* **2014**, *14(15)*, 1771–1788.

(13) Litman, R. E.; Smith, M. A.; Doherty, J. J.; Cross, A.; Raines, S.; Gertsik, L.; Zukin, S. R. AZD8529, a positive allosteric modulator at the mGluR2 receptor, does not improve symptoms in schizophrenia: A proof of principle study. *Schizophr Res*. **2016**, *172*, 152–157.

(14) Addex Therapeutics. Addex Reports Top-line Data from a Successful Phase 2a Clinical Study with ADX71149 in Schizophrenia Patients, **2015.**

https://www.addextherapeutics.com/en/news-and-events/press-releases/addex-reports-top-line-data-successful-phase-2a-clinical-study-adx71149-schizophrenia-patients/ accessed on 27 February, 2018.

(15) Kent, J. M.; Daly, E.; Kezic, I.; Lane, R.; Lim, P.; De Smedt, H.; De Boer, P.; Van Nueten, L.; Drevets, W. C.; Ceusters, M. Efficacy and safety of an adjunctive mGlu2 receptor positive allosteric modulator to a SSRI/SNRI in anxious depression. *Prog Neuropsychopharmacol Biol. Psychiatry*. **2016**, *67*, 66–73.

(16) Addex Reports top-line data from ADX71149 phase 2a study in patients with major depressive disorder (MDD) with significant anxiety symptoms. http://www.addextherapeutics.com/investors/press-releases/news-details/article/addex-reports-top-line-data-fromadx71149-phase-2a-study-in-patients-with-major-depressive-disorder/ accessed on 27 February, 2018.

(17) Dudkin, V. Y.; Fraley, M. E.; Wang, C.; Steen, J. Aminobenzotriazole derivatives. WO 2010114726, 2010.

(18) Beshore, D. C.; Dudkin, V. Y.; Kuduk, S. D.; Skudlarek, J. W.; Wang, C. Biaryl benzotriazole derivatives. WO 2010141360, 2010.

(19) Dudkin, V. Y.; Fraley, M. E.; Wang, C.; Garbaccio, R. M.; Beshore, D. C.; Kuduk, S. D.; Skudlarek, J. W. Ether benzotriazole derivatives. WO 2011022312, 2011.

(20) Tresadern, G,; Cid, J. M.; Macdonald, G. J.; Vega, J. A.; de Lucas, A. I.; García, A.; Matesanz, E.; Linares, M. L.; Oehlrich, D,; Lavreysen, H.; Biesmans, I.; Trabanco, A. A.

Scaffold hopping from pyridones to imidazo[1,2-a]pyridines. New positive allosteric modulators of metabotropic glutamate 2 receptor. *Bioorg. Med. Chem. Lett*. **2010**, *20*, 175-179.

(21) Cid, J. M.; Tresadern, G.; Duvey, G.; Lütjens, R.; Finn, T.; Rocher, J-P.; Poli, S.; Vega, J. A.; de Lucas, A. I.; Matesanz, E.; Linares, M. L.; Andrés, J. I.; Alcazar, J.; Alonso, J. M.; Macdonald, G. J.; Oehlrich, D.; Lavreysen, H.; Ahnaou, A.; Drinkenburg, W.; Mackie, C.; Pype, S.; Gallacher, D.; Trabanco, A. A. Discovery of 1‑butyl-3-chloro-4-(4-phenyl-1-piperidinyl)-(1H)‑pyridone (JNJ-40411813): A novel positive allosteric modulator of the metabotropic glutamate 2 receptor. *J. Med. Chem.* **2014**, *57*, 6495–6512.

(22) Lavreysen, H.; Ahnaou, A.; Drinkenburg, W.;Langlois, X.; Mackie, C.; Pype, S.; Lütjens, R.; Le Poul, E.; Trabanco, A. A.; Nuñez, J. M. Pharmacological and pharmacokinetic properties of JNJ-40411813, a positive allosteric modulator of the mGlu2 receptor. *Pharmacol. Res. Perspect.* **2015**, *3*, e00096.

(23) Ferenczy, G .G.; Keserű, G .M. How are fragments optimized? A retrospective analysis of 145 fragment optimizations. *J Med Chem*. **2013**, *56*, 2478–2486.

(24) Hopkins, A. L.; Keserű, G. M.; Leeson, P. D.; Rees, D. C.; Reynolds, C. H. The role of ligand efficiency metrics in drug discovery. *Nat. Rev. Drug. Discov*. **2014**, *13*, 105–121.

(25) Verdonk, M. L.; Rees, D. C. Group efficiency: a guideline for hits-to-leads chemistry. *ChemMedChem.* **2008**, *3*, 1179–1180.

(26) Hung, A. W.; Silvestre, H. L.; Wen, S.; George, G. P.; Boland, J.; Blundell, T. L.; Ciulli, A.; Abell, C. Optimization of inhibitors of mycobacterium tuberculosis pantothenate synthetase based on group efficiency analysis. *ChemMedChem*. **2016**, *11*, 38–42.

TABLES

Table 1. Functional activity and metabolic stability data of compounds **10-19**, optimized along vector 1.

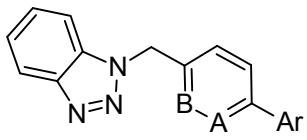

Cmpd	A	B	Ar	clogP[a]	LE	mGluR2 PAM EC_{50}±STD (nM)[b]	Cl_{int} (mL/min·g liver)[c]		
							human	rat	mouse
10	CH	CH	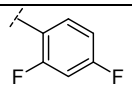	5.08	0.42	71±15	0.9	6.4	2.3
11	CH	CH	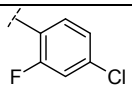	5.54	0.45	28±13	0.4	1.3	1.1
12	CH	CH	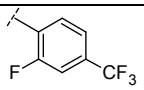	5.82	0.38	29±6	0.1	0.4	1.2
13	CH	CH	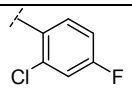	5.54	0.41	118±27	0.7	2.6	1.5
14	CH	CH	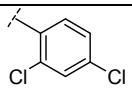	6.00	0.42	79±26	0.6	1.4	1.3
15	CH	CH	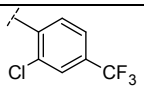	6.28	0.39	37±2	0.0	0.5	0.4
16	N	CH	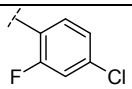	4.71	0.43	50±7	0.01	0.8	3.4
17	N	CH	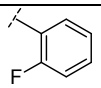	4.11	0.38	600	ND	ND	ND
18	N	CH	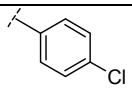	4.57	0.44	70	0.2	1.0	3.8

19	CH	N	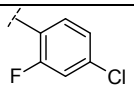	4.41	0.40	141±38	0.8	2.3	1.6

[a]clogP calculated with ChemAxon software; [b]EC_{50} values were obtained from three independent experiments; [c]Intrinsic clearance (Cl_{int}) was determined as a rate of compound consumption under first order kinetic conditions using human, rat and mouse liver microsomes; ND, not determined.

Table 2. Physicochemical properties, off target activities, and ADME parameters of **16** and **60**

Property		**16**	**60**
Physicochemical			
MW (Da)		417.67	255.24
logD (pH 7.4, calculated)		5.48	3.08
tPSA (A^2)		40.32	30.71
aqueous solubility (μg/mL, pH 7.4, measured)		3	409
Off target activities (Affinity@10 μM)[a]			
Sodium Channel, Site 2 (%)		50	ND
Androgen (Testosterone) AR (%)		77	ND
ADME			
Papp (nm/s) inward		13.4	44.4
PDR		0.8	0.7
Plasma protein binding, (bound (%))	Mouse	99.2	85.5
	Rat	99.4	90
CYP450 inhibition ($IC_{50,}$ μM)	1A2	> 10	> 10
	2D6	> 10	> 10
	2C9	6.6	> 10
	3A4	> 10	> 10
CYP induction (MEC for PXR activation, μM)		7.7	7.0

[a]The Eurofins selectivity screen was performed on the LeadProfilingScreen® (total # of assays 68); ND, not determined.

Table 3. Functional activity and metabolic stability data of compounds **24-29** along vector 2.

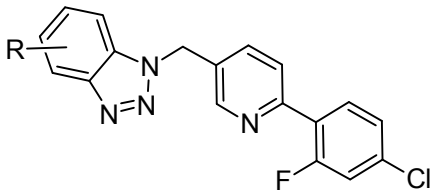

Cmpd	R	clogP[a]	LE	mGluR2 PAM EC_{50}±STD (nM)[b]	Cl_{int} (mL/min·g liver)[c]		
					human	rat	mouse
24	4-F	4.85	0.43	27±5	0.1	0.6	2.2
25	5-F	4.85	0.41	68±15	0.1	0.5	0.7
26	6-F	4.85	0.40	86±22	0.1	1.0	2.2
27	4-CN	4.57	0.41	33±12	0.05	0.1	1.6
28	4-CF_3	5.59	0.40	13±3	0.04	0.2	0.1
29	4-Br	5.48	0.47	6±4	0.1	0.4	3.8

[a]clogP calculated with ChemAxon software; [b]EC_{50} values were obtained from three independent experiments; [c]Intrinsic clearance (Cl_{int}) was determined as a rate of compound consumption under first order kinetic conditions using human, rat and mouse liver microsomes.

Table 4. Functional activity and metabolic stability data of compounds **30-41**.

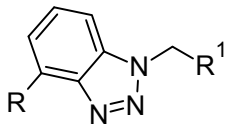

Cmpd	R	R^1	clogP[a]	LE	mGluR2 PAM EC_{50}±STD (nM)[b]	Cl_{int} (mL/min·g liver)[c]		
						human	rat	mouse
4	H	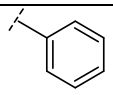	3.15	0.49	3000±720	7.9	1.2	1.1
30	Br	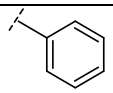	3.92	0.59	80±22	4.7	2.0	2.3
31	Br	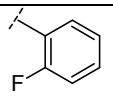	4.06	0.56	64±14	0.2	1.8	1.7
32	Br	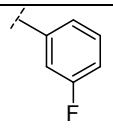	4.06	0.61	18±5	1.8	1.6	1.3
33	Br	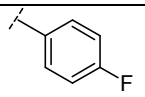	4.06	0.62	15±6	1.2	1.0	1.0
34	Br	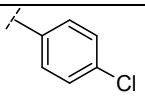	4.52	0.61	17±4	0.6	2.2	2.0
35	Br	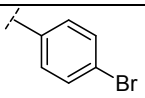	4.69	0.62	14±4	0.4	2.2	2.6
36	Br	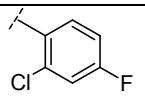	4.66	0.50	190±81	1.8	3.5	3.0
37	Br	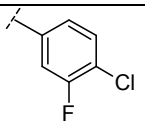	4.66	0.58	18±2	0.4	3.1	2.2
38	Br	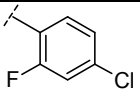	4.66	0.57	23±8	0.5	3.8	1.3

39	Br	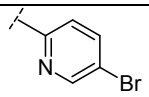	3.55	0.53	180±32	0.3	0.7	1.1
40	Br	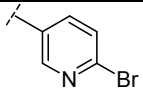	3.67	0.52	210±86	ND	ND	ND
41	Br	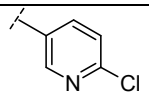	3.52	0.51	290±36	ND	ND	ND

[a]clogP calculated with ChemAxon software; [b]EC_{50} values were obtained from three independent experiments; [c]Intrinsic clearance (Cl_{int}) was determined as a rate of compound consumption under first order kinetic conditions using human, rat and mouse liver microsomes; ND, not determined.

Table 5. Functional activity and metabolic stability data of compounds **42-50**.

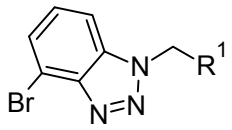

Compound	R^1	clogP[a]	LE	mGluR2 PAM EC_{50}±STD (nM)[b]	Cl_{int} (mL/min·g liver)[c]		
					human	rat	mouse
42	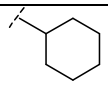	4.31	0.67	10±1	11.9	16.2	15.3
43	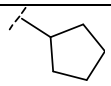	3.86	0.67	30±10	7.9	14.6	11.4
44		3.42	0.73	20±6	8.7	12.0	11.4
45		2.97	0.72	70±7	1.3	0.6	7.7
46		3.44	0.69	140±59	4.2	4.0	3.5
47	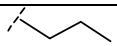	3.52	0.73	60±17	9.5	4.4	8.3
48		3.07	0.72	270±100	4.7	0.8	7.7
49		2.55	0.67	2240±549	ND	ND	ND
50	H	2.19	<0.68	>5000	ND	ND	ND

[a]clogP calculated with ChemAxon software; [b]EC_{50} values were obtained from three independent experiments; [c]Intrinsic clearance (Cl_{int}) was determined as a rate of compound consumption under first order kinetic conditions using human, rat and mouse liver microsomes; ND, not determined.

Table 6. Functional activity and metabolic stability of compounds **51-60**.

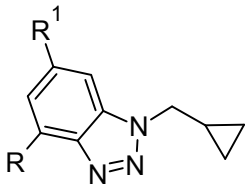

Cmpd	R	R^1	clogP[a]	LE	mGluR2 PAM EC_{50}±STD (nM)[b]	Cl_{int} (mL/min·g liver)[c]		
						human	rat	mouse
45	Br	H	2.97	0.72	70±7	1.3	0.6	7.7
51	Br	CF_3	3.85	0.54	140±48	0.1	0.2	7.7
52	Br	Br	3.74	0.69	50±12	0.6	2.3	15.3
53	Br	Cl	3.58	0.68	60±17	0.5	1.1	11.4
54	Br	F	3.12	0.70	70±11	0.4	0.5	5.7
55	Br	MeO	2.82	0.54	730±33	ND	ND	ND
56	Cl	H	2.81	0.71	90±24	4.2	0.5	5.7
57	F	H	2.35	0.60	1070±252	ND	ND	ND
58	CN	H	2.06	0.58	620±233	ND	ND	ND
59	MeO	H	2.05	0.60	400±160	1.8	0.8	8.3
60	CF_3	H	3.08	0.57	148±35	0.3	0.3	1.4

[a]clogP calculated with ChemAxon software; [b]EC_{50} values were obtained from three independent experiments; [c]Intrinsic clearance (Cl_{int}) was determined as a rate of compound consumption under first order kinetic conditions using human, rat and mouse liver microsomes; ND, not determined.

FIGURES, SCHEMES/STRUCTURES, AND CHARTS

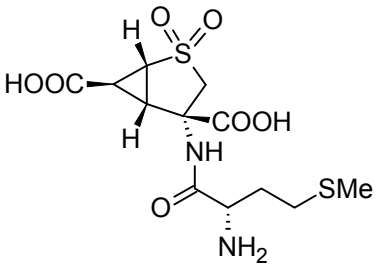

1 LY2140023 (Pomaglumetad methionil)

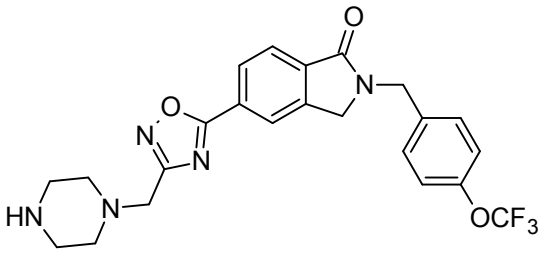

2 AZD8529

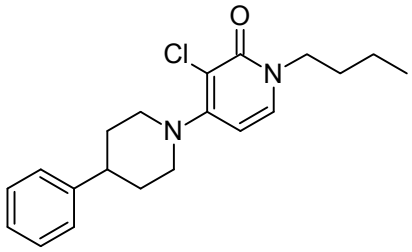

3 ADX71149 (JNJ-40411813)

Figure 1. Clinical mGluR2/3 agonist (**1**) and mGluR2 PAMs (**2** and **3**)

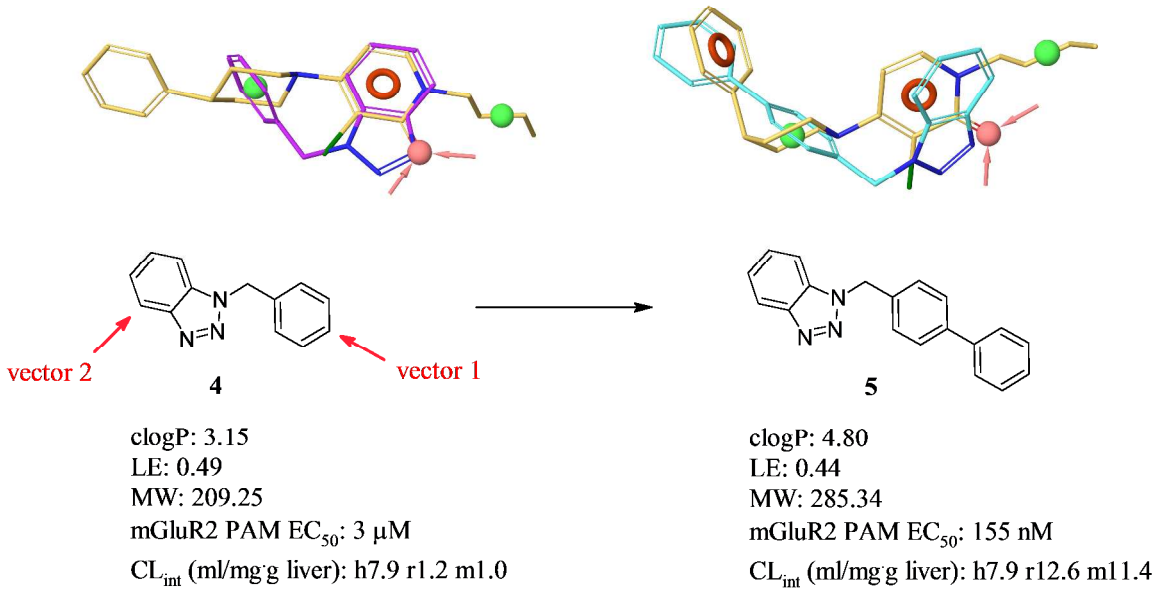

Figure 2. Identification of the chemical starting point **4** and its growing vectors leading to the biaryl-benzotriazole **5 (**blue) advanced hit. Growing vectors were based on the alignment of **4** (purple) to **3**[21,22] (yellow), a reference mGluR2 PAM.

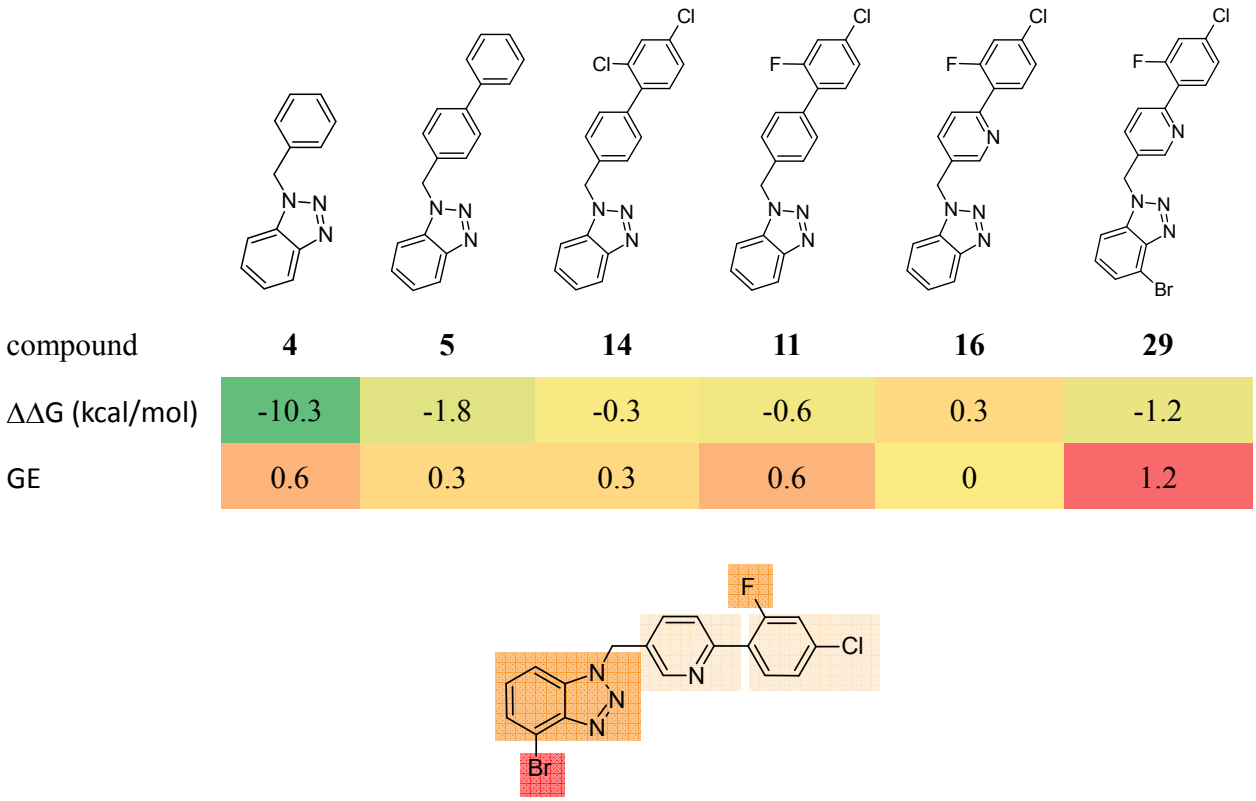

Figure 3. Group efficiency analysis of **29**. GE values are colour-coded according to the relative contribution to the binding free energy (green to red for small to large).

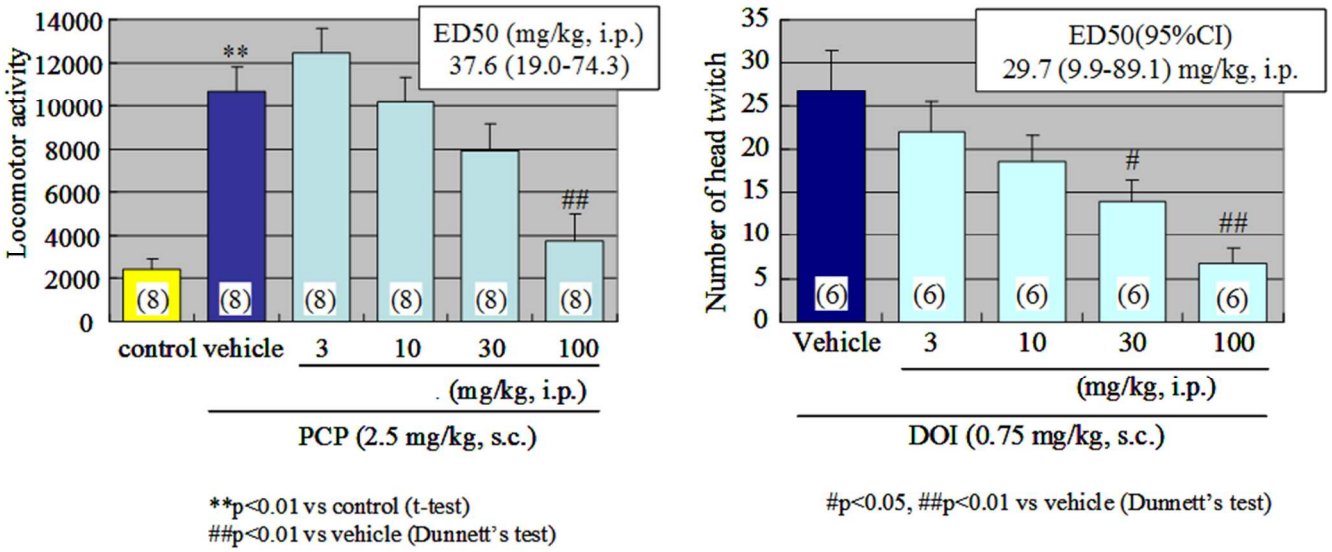

Figure 4. *In vivo* efficacy of **60** in the PCP-induced hyperlocomotion and the DOI-induced head twitch models.

Scheme 1. Synthesis of unsubstituted benzotriazoles[a]

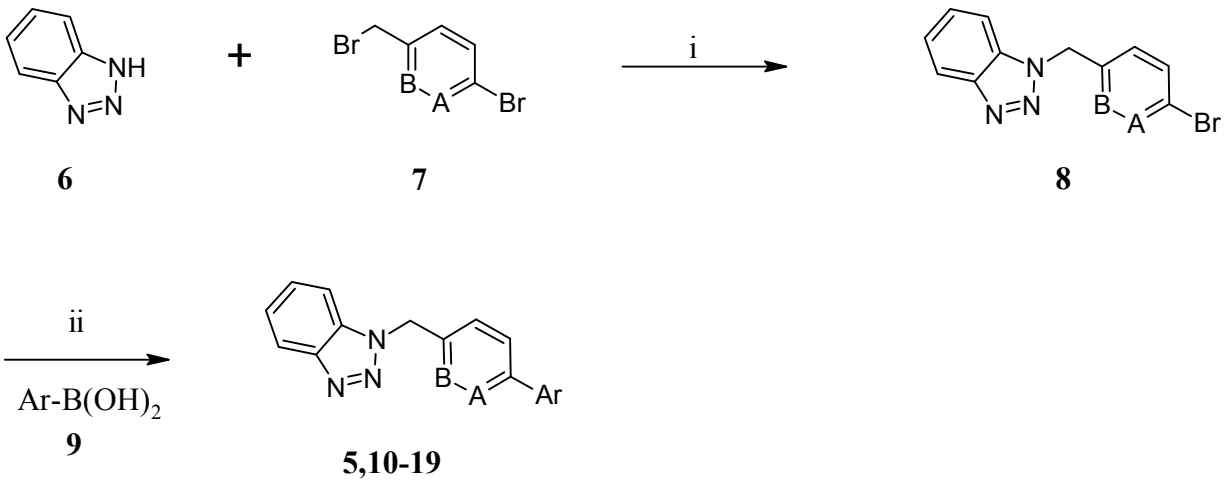

6 **7** **8** **9** **5,10-19**

[a]Reagents and conditions: (i) THF, NaHMDS, -30 ^{o}C–rt, 2h, 35–40% yield; (ii) Toluene/EtOH/H_2O, $Pd(PPh_3)_4$, Na_2CO_3, reflux, 2h, 75–90% yield.

Scheme 2. Synthesis of substituted benzotriazoles[a]

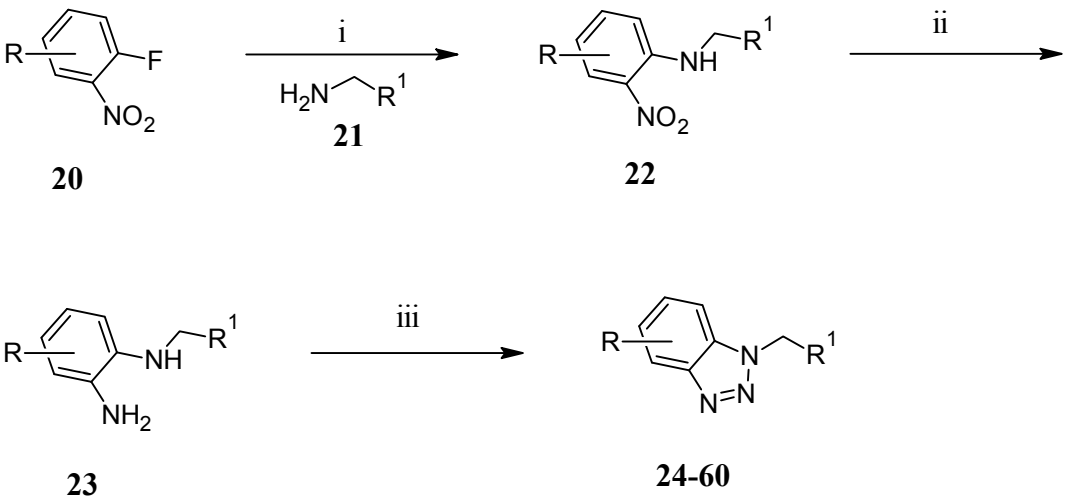

[a]Reagents and conditions: (i) AcCN, K_2CO_3, rt, 18h, 74–90% yield; (ii) MeOH/H_2O, $SnCl_2$, cc. HCl, 50 ^oC, 12h, 52–65% yield; (iii) AcOH, $NaNO_2$, 60^oC, 3h, 32–73% yield.

Table of Content graphic